The Journal of Chemical Physics

The structure of $PbCl_2$ on the {100} surface of NaCl and its consequences for crystal growth

Cite as: J. Chem. Phys. **148**, 144703 (2018); https://doi.org/10.1063/1.5026455
Submitted: 20 February 2018 . Accepted: 27 March 2018 . Published Online: 09 April 2018

Eleanor R. Townsend, Sander J. T. Brugman, Melian A. R. Blijlevens, Mireille M. H. Smets, Wester de Poel, Willem J. P. van Enckevort, Jan A. M. Meijer, and Elias Vlieg

The structure of $PbCl_2$ on the {100} surface of NaCl and its consequences for crystal growth

Eleanor R. Townsend,[1] Sander J. T. Brugman,[1] Melian A. R. Blijlevens,[1] Mireille M. H. Smets,[1] Wester de Poel,[1] Willem J. P. van Enckevort,[1] Jan A. M. Meijer,[2] and Elias Vlieg[1,a)]

[1]*Institute for Molecules and Materials, Radboud University, Heyendaalseweg 135, 6525 AJ Nijmegen, The Netherlands*

[2]*Akzo Nobel Industrial Chemicals, RD&I Salt, Zutphenseweg 10, 7418 AJ Deventer, The Netherlands*

(Received 20 February 2018; accepted 27 March 2018; published online 9 April 2018)

The role that additives play in the growth of sodium chloride is a topic which has been widely researched but not always fully understood at an atomic level. Lead chloride ($PbCl_2$) is one such additive which has been reported to have growth inhibition effects on NaCl {100} and {111}; however, no definitive evidence has been reported which details the mechanism of this interaction. In this investigation, we used the technique of surface x-ray diffraction to determine the interaction between $PbCl_2$ and NaCl {100} and the structure at the surface. We find that Pb^{2+} replaces a surface Na^+ ion, while a Cl^- ion is located on top of the Pb^{2+}. This leads to a charge mismatch in the bulk crystal, which, as energetically unfavourable, leads to a growth blocking effect. While this is a similar mechanism as in the anticaking agent ferrocyanide, the effect of $PbCl_2$ is much weaker, most likely due to the fact that the Pb^{2+} ion can more easily desorb. Moreover, $PbCl_2$ has an even stronger effect on NaCl {111}. *Published by AIP Publishing.* https://doi.org/10.1063/1.5026455

I. INTRODUCTION

Additives are frequently used during crystal growth[1] to control, for example, nucleation and crystal morphology,[2] to direct the outcome of chiral resolution,[3] or to prevent caking.[4] In the latter application, the additives are called anticaking agents, and for sodium chloride these are applied on a large industrial scale. Sodium chloride has for many years been a model compound of choice for investigation into the effects of additives on crystallisation, along with its sister compound potassium chloride, due to its relatively simple crystal structure and abundance in nature. In 1932, Kading[5] reported that lead ions can have a marked effect on the crystallisation of many alkali halide salts of which discovery led to many more investigations into the effect of Pb^{2+} on NaCl and KCl. Bunn and Emmett[6] suggested that Pb^{2+} causes both a decrease in step height and growth inhibition of a growing NaCl crystal, a finding which is echoed by Botsaris *et al.*[7] and Glasner and Skurnik[8] in their 1966 and 1967 articles, respectively. Both articles agree that Pb^{2+} ions retard the nucleation and subsequent growth of KCl; however, there is a disagreement between the two on the mechanism of this interaction. This growth blocking was also observed by Sears, who described the hindering of KCl growth from a supersaturated solution containing 1% $PbCl_2$.[9]

As a consequence of the growth blocking, lead ions are also known to affect the habit (i.e., growth morphology) of alkali halide crystals.[10] This was first reported by Bienfait *et al.*[11] who showed, through the use of a growth morphodrom, that Pb^{2+} significantly lowers the supersaturation needed to change the external form from {100} to {111} in NaCl. The same was found for other ions, such as Mn^{2+} and Cd^{2+}. A similar observation was seen by Li *et al.*,[12] who also described a growth morphodrom, except this time for KCl in the presence of Pb^{2+}. They described the changes in crystal habit and surface microtopographs observable dependent on the supersaturation and respective Pb^{2+} concentration, showing the eventual elucidation of {111} facets under varying additive concentrations and supersaturations.

The early experiments describe the effect of additives on a macroscopic scale. It is thus interesting to understand the mechanism of how the Pb^{2+} interacts with the {100} and {111} surfaces of NaCl on an atomic scale. Booth[13] suggested that in the case of NaCl, Pb^{2+} is incorporated along the {100} facets but not the {111}. The explanation using a variety of models was discussed by Botsaris *et al.*,[7] but no definitive experimental proof was reported. More recently, Radenovic *et al.*[14] showed the structure of the {111} NaCl crystal surface in contact with a brine solution containing $CdCl_2$ using surface x-ray diffraction (SXRD). They showed that the adsorption layer consisted of a mixed monolayer of Cd^{2+} and water with occupancies of 0.25 and 0.75, respectively, in contact with the top Cl^- layer on the {111} surface. As $CdCl_2$ was reported by Bienfait *et al.*,[11] as having a similar effect on the NaCl habit as $PbCl_2$ (i.e., change from {100} to {111} observable facets), we can assume that $PbCl_2$ would show the same mechanism. However, this does not explain the role of Pb^{2+} when it is put into contact in solution with an already formed {100} surface.

a)Electronic mail: e.vlieg@science.ru.nl

The aim of this paper is to determine the mechanism of attachment of $PbCl_2$ to the {100} surface of sodium chloride at an atomic scale. The technique of surface x-ray diffraction (SXRD) is used for this. We intend through this investigation to gain valuable insight into the mechanism of action of transition metal halides on this substrate and to create a model which describes accurately this process.

II. METHODS

The cubic NaCl crystals (a = 5.62 Å) used in this experiment were grown from a saturated sodium chloride solution, which had been filtered using 0.45 μm Whatman filters. The approximate size of the crystal used in the final experiment was $6 \times 6 \times 3$ mm^3. Evaporation was minimised by crystallising in an Erlenmeyer flask, with the opening covered with Parafilm containing a small hole. This setup also prevented contamination of the growth solution with dust or other foreign particles. After removal from the growth solution, the NaCl crystals were dried using a dust-free tissue and stored in a temperature and humidity controlled climate chamber to prevent roughening. The resulting crystals were nearly optically defect free.

In previous experiments, SXRD has been used successfully with NaCl as a substrate, both on the {100} and {111} facets. Arsic *et al.*[15] determined the ordering of the water layers on the {100} surface, which was then followed by the previously mentioned work by Radenovic *et al.*,[14] in which the influence of cadmium on the {111} surface was investigated. More recently, SXRD was also used to determine the mechanism of the anticaking activity of ferrocyanide on the {100} NaCl surface.[16] With SXRD, the diffracted intensity is measured along the so-called crystal truncation rods (CTRs).[17,18] These rods consist of out-of-plane tails of diffracted intensity connecting bulk Bragg peaks and are sensitive to the interface structure.

The SXRD experiments for this investigation were performed at the MS-X04SA beamline[19] at the Swiss Light Source (SLS) in the Paul Scherrer Institute in Villingen, Switzerland. The radiation used had a photon energy of 20 keV, corresponding to a wavelength of 0.62 Å, and a beam size of 60×1000 μm^2. The measurements were taken using a vertical (2 + 2) type diffractometer with a PILATUS area detector at an incidence angle of 0.6°. Complementary experiments were performed prior to this at the Diamond Light Source in Didcot, U.K. In this paper, we only show the more extensive results from the SLS, but the data from the Diamond Light Source were very similar, proving the reproducibility of the experiments.

We measured data sets for NaCl {100} treated with a solution of $PbCl_2$. The solution consisted of a slightly undersaturated solution of brine containing varying amounts of $PbCl_2$, which was subsequently filtered using a 0.2 μm Whatman filter. The data which we obtained and analyzed in this paper were gathered using a solution that is 95% saturated with NaCl to which 10 g/l $PbCl_2$ is added. The concentration of Pb in the solution is then 3.6×10^{-2} mol/l, which corresponds to approximately 2×10^{16} ions Pb^{2+}/μl. At these high Cl^- concentrations, the Pb^{2+} ions are largely dissolved as $[PbCl_3]^-$ and $[PbCl_4]^{2-}$ complexes.[20]

5 μl solution was applied to the crystal surface using the following method: a dust-free tissue was pulled tightly across the crystal surface and then a droplet is applied to this and allowed soaking in for a few seconds before removal. This method was employed to minimise the height of the liquid layer present on the crystal surface and prevent roughening of the surface. The crystal was then immediately placed into the setup, which consisted of an isolated cell at room temperature, in which the relative humidity was regulated at 75%. This humidity was regulated by the presence of a saturated solution of NaCl in the environment. By using this method, we found that roughness was minimised on the NaCl surface and also there was no presence of a thick liquid layer which would impede our measurements by giving a strong background signal. However, as this is just at the deliquescence point of NaCl, there is definitely a water layer present.[21] Other measurements which were performed used different initial $PbCl_2$ concentrations and were also analyzed for the discussion of this article.

In order to fully derive the surface structure, a data set of different rods is necessary. The momentum transfer $\vec{Q}$ is dependent on the diffraction indices hkl and the reciprocal lattice vectors $\vec{b_i}$,

$$\vec{Q} = h\vec{b_1} + k\vec{b_2} + l\vec{b_3}.$$

We orient the unit cell such that the direction perpendicular to the surface is denoted by l, and h and k denote the directions that are parallel to the a and b axes, respectively. Therefore we are technically studying the (001) surface of NaCl. A MATLAB script was used to convert the data into structure factors, applying the necessary correction factors.[22] Model calculations and fitting were performed using the program ROD.[23] The contribution of the data points close to the Bragg peak was weighted to give a 30% larger error bar, in order to increase the weight of the surface sensitive data points.

III. RESULTS

The data set consists of 401 non-equivalent reflections, relating to the (00), (11), (13), (20), and (22) rods. The full data set that was measured also included the rods $(1\bar{1})$, $(1\bar{3})$, (02), and $(2\bar{2})$, which was then averaged to give the final data set which had an agreement factor of 12%. The data are shown in Fig. 1 as blue dots, together with the calculated profile for an ideal NaCl (001) surface (dashed curves). It is clear that the data deviate strongly from this and also from the data on NaCl (001) in water.[15] From this, we conclude that the $PbCl_2$ must have a well-defined location at the surface. There are two simple configurations in which the $PbCl_2$ could be located at the surface: either embedded in the top NaCl layer or on top of this. These two different models, shown in Fig. 2, are hereby named "*embed*" and "*surface*."

The first model, *embed*, was inspired by the models from the studies of Arsic[15] and Bode.[16] Bode placed ferrocyanide ions into the surface, positioned with the iron atom at the sodium ion location and five cyanide ligands replacing the chlorines surrounding the sodium atom and one cyanide ligand sticking out perpendicular to the surface. In *embed*, the first

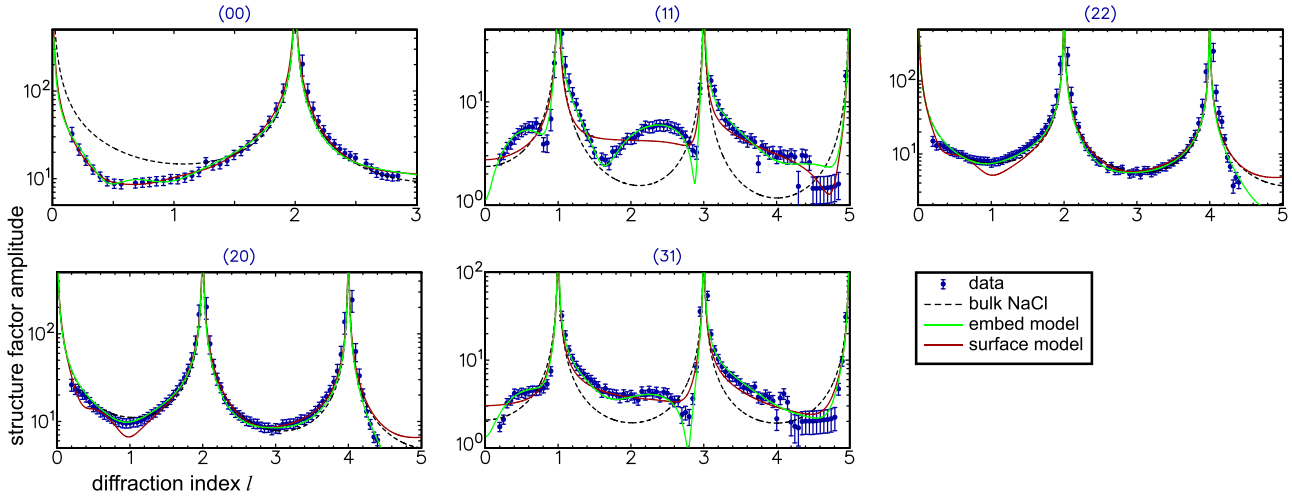

FIG. 1. The measured rods of NaCl(100) (blue dots with error bars) together with fits to the models *embed* (green curves) and *surface* (red curves). For comparison, the rods calculated for an ideal (100) surface are shown as dashed curves.

surface layer consists of chlorine and sodium ions, with some sodium positions being substituted with a lead ion. This gives the surface structure shown in Fig. 2(a). In order to balance the extra positive charge of the lead ion, we placed a chlorine ion directly above the positions where lead is present. The rest of the empty positions in the second layer are occupied with oxygen atoms. In the case of these models, oxygen is used to describe the locations of water molecules, as hydrogen is invisible in these SXRD measurements, due to its low electron density.

The second model, *surface*, is inspired by the findings of Radenovic[14] on the {111} surface, where the ions are in contact with the upper layer of the NaCl surface, but do not replace atoms as in the *embed* model. In this model, lead atoms are located above the chlorine positions of the first NaCl bulk layer. The charge of the lead is compensated with two chlorine atoms in the same layer, the rest of which is then filled with oxygen atoms representing water molecules. This model is explained diagrammatically in Fig. 2(b).

In both models, we consider two types of oxygen units directly on top of the NaCl surface. Atom O1a is placed directly on a Na^+ ion, and O1b is placed above a Cl^- ion. We find that these two different locations are needed to obtain a good fit. Previous SXRD studies on the NaCl(100) surface[15,16] only considered O (i.e., water) on top of Na, but the larger data set used here is more sensitive to these structural details. Additional water layers are expected to be increasingly disordered as they are located further away from the interface. Here we use one extra water layer, O2, plus a water film with the density of a saturated NaCl solution to accurately describe the water layering, as observed earlier.[15] Under the experimental conditions of 75% relative humidity, the total water film thickness is approximately 40 Å.[21]

In order to determine the optimum fit, the data set was fitted using a χ^2 minimisation routine, in which the position and occupancies of the various atoms in the models are varied. Due to the similarities in the ionic radius between Pb^{2+} (1.19 Å[24]) and Na^+(1.02 Å[24]), we do not expect that a large surface reconstruction is necessary to incorporate the Pb^{2+} ion into the NaCl lattice structure. In addition, no evidence for long-range ordered surface reconstruction, manifesting as extra, higher order peaks in the x-ray diffraction rod patterns, was found. Therefore, we will only consider a normal 1×1 unit cell, as indicated in Fig. 2.

The interface region is built upon the upper layers of bulk sodium chloride, as shown in Fig. 2. We tested several variations of the models, with varying number of fitting parameters. Here we report the result of the simplest models in which the topmost NaCl layer is fully occupied and no vertical relaxation in the position of ions Cl1 and Na1 is included. Such relaxations were found to be very small on the clean surface.[15] Where applied, fit parameters were used in the vertical positions only, as we expect the horizontal positions to largely retain the bulk positions. Furthermore, Debye-Waller parameters were fitted, to allow for disorder in both the in-plane and out-of-plane directions. These values help us to indicate low levels of relaxation in the horizontal direction, if present. It was not necessary to incorporate a roughness parameter into our model, and this indicates that we had a very high-quality surface before and during the experiment.

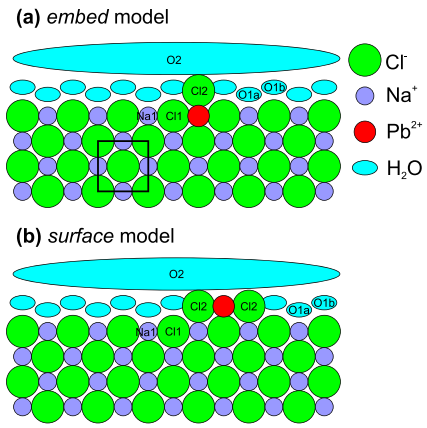

FIG. 2. Side views of the models used to fit the data: (a) *embed* and (b) *surface*. The conventional fcc unit cell is indicated by the black square (a = 5.62 Å).

TABLE I. Summary of the best fit parameters for the data set using the model *embed*. z values are described with respect to the topmost NaCl layer. * denotes the constrained parameters.

Atom	Occupancy	z (Å)	$DW_{\parallel}$ (Å^2)	$DW_{\perp}$ (Å^2)
O2	1.8 ± 0.2	6.3 ± 0.3	∞	490 ± 50
O1b	1.4 ± 0.1	3.0 ± 0.3	11 ± 2	90 ± 10
O1a	1.0 ± 0.1	2.6 ± 0.1	40 ± 5	7 ± 2
Cl2	0.10*	2.9 ± 0.2	1 ± 0.5	1 ± 0.5
Pb1	0.10 ± 0.02	0.4 ± 0.2	7 ± 2	3 ± 1
Cl1	≡1	≡0	2 ± 0.5	2 ± 0.5
Na1	0.90*	≡0	2 ± 0.5	2 ± 0.5

The data fitted to the model *embed* are shown in Fig. 1 (green curves), with the corresponding parameters shown in Table I. The agreement is excellent, with a final reduced χ^2 value of 1.39. Some occupancies were constrained in relation to each other, as they are dependent on each other to achieve the expected full coverage of the NaCl surface and charge neutrality. These are indicated in Table I with an asterisk. We assume therefore

$$\text{Occupancy(Cl2)} = \text{Occupancy(Pb)},$$

$$\text{Occupancy(Na1)} = 1 - \text{Occupancy(Pb)}.$$

From the refined model, we can calculate the z-projected electron density for the (00) and (11) Fourier components, as shown in Fig. 3. The (00) component is only sensitive to order in the out-of-plane direction, but this is not the case for other rods, which also have an in-plane component. As we see a peak at 2.6 Å for both the (00) and (11) projections, this shows that we also have significant in-plane ordering in the first water layer, i.e., Cl2 and the water layers O1a and O1b, as well as out-of-plane. This plot also shows that above 5 Å there is very little lateral order.

The data fitted to the model *surface* are also shown in Fig. 1 as the red curves. In the case of this model, constraints were also made in relation to the occupancies of the various sites on the surface. It is clear that this model does not yield a satisfactory fit, as most clearly visible in the (11) rod, and therefore no table of fit parameters is given here. The reduced χ^2 value of 2.81 is still reasonable, but this is mainly due to the fact that the (00), (20), and (22) rods are found to be insensitive to the difference between the two models considered here. If extra layers are added, the fit of the *surface* model can be improved, but the fitting parameters are then essentially trying to mimic the *embed* model.

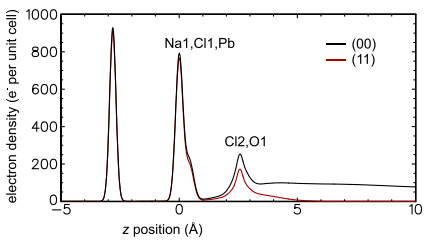

FIG. 3. The projected z-density as calculated for the (00) and (11) Fourier components from the *embed* model.

IV. DISCUSSION

Comparing the results from the fitting of both models, it is clear that the *embed* model gives a superior fit to that of the *surface* model. This follows from comparing the data and fits in Fig. 1 as well as from the much lower χ^2 value of the fit in the *embed* model. The largest discrepancies in the surface fit are observable in the (11) and (31) rods. We can therefore conclude that on the NaCl {100} surface in the presence of a $PbCl_2$ solution, Pb^{2+} ions replace some of the topmost Na^+ ions, at a slightly higher position (0.4 Å) that partly reflects the larger size of Pb^{2+}. Above each Pb^{2+} ion on the surface is a chlorine ion, which allows for charge neutralisation of the Pb^{2+} atom. The distance between Pb and Cl2 is found to be 2.5 ± 0.3 Å, which is somewhat smaller than the sum of the ionic radii, 3.0 Å. The remaining surface is covered with a layer of water. From the Debye-Waller parameters, we see that the water molecules (modeled by atoms O1a and O1b) show significant lateral disorder, indicating that these are quite mobile. From the z-density calculation, we can see that the water layers above the first water layer are hardly ordered (Fig. 3).

Our results here show an occupancy of 10% for the Pb^{2+} ion. The number of Pb^{2+} ions at this coverage on the 6×6 mm^2 NaCl surface equals 2×10^{13}, which is about a factor 5000 less than dissolved in the 5 μm solution that was applied. We may thus expect that the liquid film on the surface has a sufficient amount of Pb^{2+} ions and that the 10% occupancy corresponds to the maximum amount that can be adsorbed. This is confirmed by the presence of $PbCl_2$ crystallites on the surface, which were observed at the expected points on the specular rod by the presence of strong diffraction ring patterns. $PbCl_2$ crystallites were also observed by optical microscopy by Li *et al.*[12] The maximum occupancy of Pb^{2+} was further confirmed by the analysis of two previous experiments, one using a solution with an initial $PbCl_2$ concentration of 1.5 g/l and the other one with 0.2 g/l. The latter experiment was performed at Diamond Light Source. Upon analysis of these data, we confirmed that also here only the *embed* model gave an excellent fit. The observed occupancies for these experiments were 8% and 5%, respectively. Therefore we can say that 10% is the maximum occupancy for Pb^{2+} ions on this surface.

It is likely that the relaxation needed on the surface to incorporate the Pb^{2+} ion is relatively large (its radius is 17% larger than the smaller Na^+ ion) and is too disruptive to the surface for it to be feasible to occupy more than 10% of surface sites. A 10% occupancy corresponds with an average distance between adjacent Pb^{2+} ions of only 2.2 unit cell lengths, which is still quite close. Our SXRD measurements did not show that the Pb^{2+} positions had long-range order, but short-range order is still possible. Such order might be confirmed using atomic resolution atomic force microscopy.

Here we have determined that Pb^{2+} is embedded in the {100} surface. Given the similarity in the effects of Pb^{2+}, Cd^{2+}, and Mn^{2+} on the observed growth behavior,[11] we may assume that the mechanism for the attachment of Pb^{2+} to the NaCl {111} surface mirrors that found by Radenovic *et al.*[14] for $CdCl_2$, in which they state that a mixed 1:3 monolayer of Cd^{2+}

and water is in direct contact with the top Cl^- layers of the {111} surface below. We are thus in the special situation that we have an atomic scale picture of the interface of NaCl in the presence of Pb^{2+} for both the {100} surface and the {111} surface. Based on this, one would initially expect the embedded Pb^{2+} on the {100} surface to have a stronger blocking effect than the floating Pb^{2+} on the {111} surface.

It has long been established, however, that while there is a retardation effect of the {100} surface,[9,13] the effect on the {111} is even stronger.[11–13] This causes the {111} surfaces to grow slower than the {100} facets and thus the presence of Pb^{2+} ions in the growth solution leads to a change in growth morphology from {100} to {111} facets. Pb^{2+} thus blocks the growth steps on the {111} facets more strongly than on the {100} facets. It is unexpected that the Pb^{2+} that is floating on the {111} terraces has such a strong effect, but it may be strongly bound at step edges. A local probe-like atomic force microscopy is needed to confirm this.

The fact that the embedded Pb^{2+} is not a good step blocker is surprising, given the similarity with ferrocyanide, a well-known anticaking agent for NaCl that blocks growth steps on the {100} surface very effectively. Bode *et al.*[16] found that the ferrocyanide ion $[Fe(CN)_6]^{4-}$ replaces a $[NaCl_5]^{4-}$ cluster at the surface, rather similar to the replacement of Na^+ by $[PbCl]^+$ in our case. In both cases, the compound fits in the NaCl lattice; for ferrocyanide, the geometric mismatch is only 1%[10] and the ionic radius of Pb^{2+} is 17% larger than that of Na^+. However, in order for the crystal to continue growing, i.e., to incorporate the ferrocyanide ion into the bulk, a Na^+ vacancy must be created in order to balance the charges between $[Fe(CN)_6]^{4-}$ and $[NaCl_6]^{5-}$. This is energetically unfavourable and therefore causes growth to be blocked. A similar mechanism occurs for $PbCl_2$ but with one large exception. Unlike the large and strongly bound ferrocyanide molecule, the single Pb^{2+} ion does not necessarily have to be incorporated, but can alternatively desorb. The difference in desorption behavior is thus likely the reason why ferrocyanide is an outstanding anticaking agent for NaCl, while $PbCl_2$ is not.

In addition, the Pb^{2+} has a lower surface concentration than ferrocyanide (10% versus up to 50%[16]), but this is probably less important for the step blocking.

V. CONCLUSIONS

In this investigation, we have applied surface x-ray diffraction to study the sorption of Pb^{2+} ions on sodium chloride crystals. Using this technique, we were able to deduce a mechanism for how the Pb^{2+} ion adsorbs to the {100} facets of sodium chloride, which involves the replacement of a Na^+ ion with a Pb^{2+} ion, partially blocking the growth through an ion charge mismatch in the bulk. The blocking on the {100} facet, however, is weaker than on the {111} facet, and thus the growth morphology of NaCl changes from {100} to {111} for increasing Pb^{2+} concentrations.

ACKNOWLEDGMENTS

We acknowledge the Paul Scherrer Institut, Villigen, Switzerland for provision of synchrotron radiation beamtime at beamline MS-X04SA of the SLS and would like to thank Dr. Phil Wilmott for assistance. This work was also carried out with the support of the Diamond Light Source (Proposal No. SI11393-1) and the authors would like to acknowledge the efforts by Dr. Chris Nicklin and Dr. Jonathan Rawle. The authors would finally like to acknowledge Akzo Nobel Industrial Chemicals for funding this project.

[1] K. Sangwal, *Additives and Crystallisation Processes: From Fundamentals to Applications* (Wiley, 2007).
[2] I. Weissbuch, L. Addadi, M. Lahav, and L. Leiserowitz, Science **253**, 637 (1991).
[3] A. H. J. Engwerda, P. van Schayik, H. Jagtenberg, H. Meekes, F. P. J. T. Rutjes, and E. Vlieg, Chem. Eur. J. **24**, 2863 (2018).
[4] D. Kaufmann, *Sodium Chloride: The Production and Propoerties of Salt and Brine* (Reinhold Publishing Corporation, 1960).
[5] H. Kading, Z. Phys. Chem. **162**, 174 (1932).
[6] C. W. Bunn and H. Emmett, Discuss. Faraday Soc. **5**, 119 (1949).
[7] G. Botsaris, E. A. Mason, and R. C. Reid, J. Chem. Phys. **45**, 1893 (1966).
[8] A. Glasner and S. Skurnik, J. Chem. Phys. **47**, 3687 (1967).
[9] G. W. Sears, J. Chem. Phys. **29**, 979 (1958).
[10] A. Glasner, Isr. J. Chem. **7**, 633 (1969).
[11] M. Bienfait, R. Boistelle, and R. Kern, *Adsorption et Croissance Cristalline* (Centre National de la Recherche Scientifique, Paris, 1965).
[12] L. Li, K. Tsukamoto, and I. Sunagawa, J. Cryst. Growth **99**, 150 (1990).
[13] A. H. Booth, Trans. Faraday Soc. **47**, 633–640 (1951).
[14] N. Radenovic, W. J. P. van Enckevort, D. Kaminski, M. Heijna, and E. Vlieg, Surf. Sci. **599**, 196 (2005).
[15] J. Arsic, D. Kaminski, N. Radenovic, P. Poodt, W. Graswinckel, H. Cuppen, and E. Vlieg, J. Chem. Phys. **120**, 9720 (2004).
[16] A. A. C. Bode, V. Vonk, F. J. van den Bruele, D. J. Kok, A. M. Kerkenaar, M. F. Mantilla, S. Jiang, J. A. M. Meijer, W. J. P. van Enckevort, and E. Vlieg, Cryst. Growth Des. **12**, 1919 (2012).
[17] I. K. Robinson, Phys. Rev. B **33**, 3830 (1986).
[18] E. Vlieg, in *Surface and Interface Science: Concept and Methods* (Wiley-VCH, 2012), Vol. 1, Chap. 3.4.2, pp. 375–425.
[19] P. R. Willmott, D. Meister, S. J. Leake, M. Lange, A. Bergamaschi, M. Boge, M. Calvi, C. Cancellieri, N. Casati, A. Cervellino, Q. Chen, C. David, U. Flechsig, F. Gozzo, B. Henrich, S. Jaggi-Spielmann, B. Jakob, I. Kalichava, P. Karvinen, J. Krempasky, A. Ludeke, R. Luscher, S. Maag, C. Quitmann, M. L. Reinle-Schmitt, T. Schmidt, B. Schmitt, A. Streun, I. Vartiainen, M. Vitins, X. Wang, and R. Wullschleger, J. Synchrotron Radiat. **20**, 667 (2013).
[20] T. Seward, Geochim. Cosmochim. Acta **48**, 121 (1984).
[21] N. Radenovic, D. Kaminski, W. van Enckevort, W. Graswinckel, I. Shah, M. in t Veld, R. Algra, and E. Vlieg, J. Chem. Phys. **124**, 164706 (2006).
[22] E. Vlieg, J. Appl. Cryst. **30**, 532 (1997).
[23] E. Vlieg, J. Appl. Cryst. **33**, 401 (2000).
[24] A. F. Wells, *Structural Inorganic Chemistry* (Clarendon Press, 1984), Vol. 5.